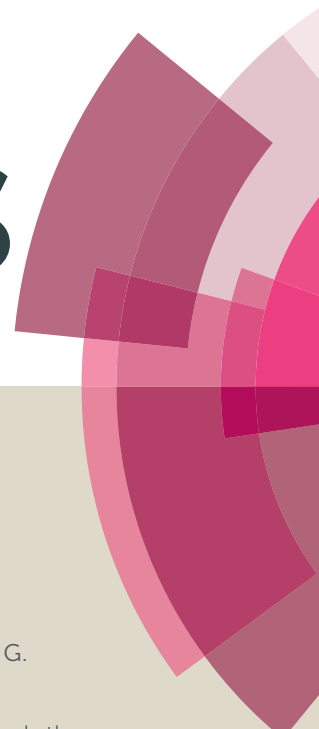
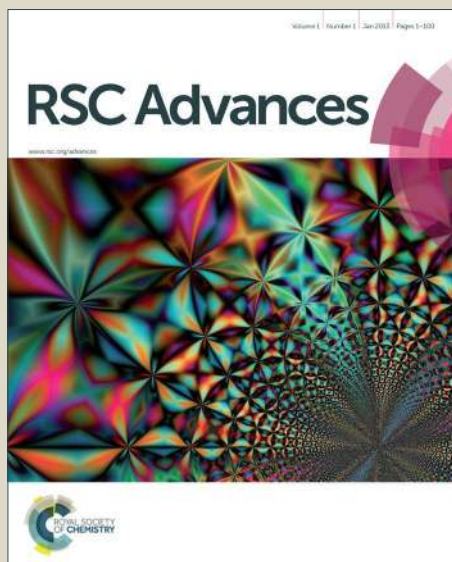


RSC Advances



This article can be cited before page numbers have been issued, to do this please use: P. R. Bhagat, A. G. Khiratkar and S. S., *RSC Adv.*, 2016, DOI: 10.1039/C6RA01219A.



This is an *Accepted Manuscript*, which has been through the Royal Society of Chemistry peer review process and has been accepted for publication.

Accepted Manuscripts are published online shortly after acceptance, before technical editing, formatting and proof reading. Using this free service, authors can make their results available to the community, in citable form, before we publish the edited article. This *Accepted Manuscript* will be replaced by the edited, formatted and paginated article as soon as this is available.

You can find more information about *Accepted Manuscripts* in the [Information for Authors](#).

Please note that technical editing may introduce minor changes to the text and/or graphics, which may alter content. The journal's standard [Terms & Conditions](#) and the [Ethical guidelines](#) still apply. In no event shall the Royal Society of Chemistry be held responsible for any errors or omissions in this *Accepted Manuscript* or any consequences arising from the use of any information it contains.



ARTICLE

Designing of sulphonic acid functionalized benzimidazolium based poly(ionic liquid) for efficient adsorption of hexavalent chromium

Avinash Ganesh Khiratkar, S. Senthil Kumar and Pundlik Rambhau Bhagat*

Received 00th January 20xx,
Accepted 00th January 20xx

DOI: 10.1039/x0xx00000x

www.rsc.org/

Herein, the facile synthesis of sulphonic acid functionalized benzimidazolium based poly(ionic liquid) (SBPIL) is reported for the first time and investigated its efficacy towards removal of Cr(VI). SBPIL was synthesized by co-polymerization of styrene and 1-(4-vinylbenzyl)-1H-benzimidazole, followed by reaction with 1,4-butane sultone and subsequent functionalization with sulphonic acid. The prepared SBPIL was characterized by elemental analysis, FT-IR and NMR spectra, SEM-EDAX, TGA and X-ray diffraction techniques. The batch adsorption method was applied for examining the Cr(VI) removal and also to investigate the kinetics and thermodynamics of adsorption. The adsorption process was correlated with the Langmuir and Freundlich adsorption isotherm models and the Langmuir adsorption capacity was estimated to be 40.81 mg g⁻¹. The thermodynamic study concluded that the adsorption process is exothermic and spontaneous and the adsorption kinetics was well fitted by pseudo-second order kinetic model. Investigation on the effect of counter ion on the adsorption process revealed that Cl⁻ ion had no influence on the adsorption, whereas SO₄²⁻ and NO₃⁻ were found to affect the Cr(VI) adsorption by 3.6% and 19.5% respectively. SBPIL exhibited excellent stability and recyclability and the adsorbent could be easily regenerated using 1 M H₂SO₄ and examined for Cr(VI) removal from successive batches.

Introduction

Removal of chromium compounds is considered to be a highly preferred process since they are hazardous inorganic water pollutants causing danger to human beings and the environment by its mutagenicity and carcinogenic properties as well as it causes internal hemorrhage, nausea, diarrhea, liver and kidney damage.¹ Chromium compounds are released into water body through the effluents of industries like automobile, tannery, textile, ink manufacturing and many more.² Cr(III) and Cr(VI) compounds are mainly occurring in the environment whereas the +1, +4 and +5 states are rare. Cr(III) is much less toxic than Cr(VI) and essential element in humans. Hence, it is mandatory that wastewater containing Cr(VI) has to be treated before being released into the environment.

Though various techniques such as precipitation,³ solvent extraction^{4,5} and activated charcoal treatment⁶ are investigated towards the removal of toxic metal ions, adsorption over specific solid adsorbents is highly preferred as it can be carried out with low investment and minimum space.^{7,8} Accordingly, adsorption process is extensively used for the treatment of industrial wastewater from organic and inorganic pollutants based on which it has attracted immense interest among researchers.^{9,10}

In the recent past, ionic liquids (ILs) have been explored as

suitable materials in water treatment owing to their high ionic conductivity, polarity and thermal stability.^{11,12} Moreover, the functionality (both cations and anions) of these ILs are tuneable and this makes them as interesting candidates towards the extraction of metal ions from aqueous solutions and the extraction occurs often via an ion-exchange mechanism.¹³⁻¹⁸ However, loss of ionic liquid components during the extraction process would hamper the regeneration of the ILs. In addition, some of these components such as PF₆⁻ may hydrolyze to yield toxic and corrosive products and this results in contamination of water.^{19,20} Though an extraction of metal ions using ILs could be achieved successfully, contamination of water by the IL components and its products are unlikely. This shortcoming could be overcome by the immobilization of ILs on a solid support and the ion-exchange characteristic of the ILs could be effectively used for efficient adsorption of metal ions.²¹ However, immobilization of ILs on solid support needs tedious procedures and also it is challenging to have a controlled/ uniform distribution of ILs on these solid supports, which is essential for the reproducibility. Poly ionic liquids (PILs) with comparatively better processability than the corresponding monomers could be explored as suitable solid adsorbents.²² Here, the ion-exchange can occur without the leaching of any IL components into the aqueous solution. Additionally, the PILs can be made hydrophobic by metathesis with hydrophobic counter-ions and this allows easy removal of metal ions from aqueous solution by the facile heterogeneous regime.

In the present investigation, we have synthesized a sulphonic acid functionalized benzimidazolium based poly (ionic liquid) (SBPIL) and applied towards the removal of Cr(VI) ions. The structure and physicochemical properties of the SBPIL were investigated

Department of Chemistry, School of Advanced Sciences, VIT University, Vellore-632014, India.

† Electronic Supplementary Information (ESI) available: ¹H NMR and FTIR spectra, XRD pattern and Thermogram of SBPIL, 1-(4-vinylbenzyl)-1H-benzimidazole. See DOI: 10.1039/x0xx00000x

thoroughly. The kinetic and thermodynamic investigation of the adsorption was studied by examining the effect of pH, time, dose and temperature for the adsorption of Cr(VI).

Experimental

Materials

4-vinylbenzyl chloride (90%), styrene (99.99%) and 1,4-butane sultone were purchased from Sigma-Aldrich, USA. Azobisisobutyronitrile (AIBN), sulphuric acid, hydrochloric acid, potassium chloride, sodium sulphate and potassium nitrate were obtained from Avra Synthesis, India. Sodium hydride (60% suspension in paraffin oil), potassium dichromate and chloroform were procured from S D Fine-Chem, India. Acetonitrile, tetrahydrofuran (especially dried), methanol, diethyl ether and benzimidazole were purchased from LOBA Chemie, India. A stock solution of 1000 mg L⁻¹ was prepared by the diluting appropriate amount of potassium dichromate salt in 1000 mL milli-Q water. Working solutions were prepared by proper dilutions.

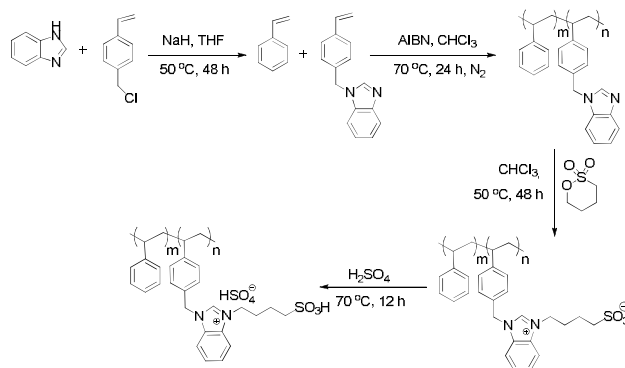
Instrumentation

NMR spectra were recorded in DMSO-*d*₆ and CDCl₃ on Bruker spectrometer operating at 400 MHz and chemical shifts are given in ppm downfield from TMS ($\delta=0.00$). Surface morphology and the elemental composition of the adsorbent were investigated using scanning electron microscope (SEM) along with energy dispersive X-ray (EDX) spectroscopy (Carl Zeiss EVO/18SH, UK). An accelerating voltage of 10 kV was applied to obtain SEM images. The sample was coated over carbon tape and gold particles were sputtered over the sample using gold sputter coater, after which the polymeric material was directly analyzed using the scanning electron microscope. FT-IR spectra of the adsorbent were obtained from IR affinity-1 Shimadzu FT-IR spectrophotometer using KBr pellet method. Elemental analyses (C, H, N, O and S) were carried out using a EURO VECTOR EA 3000 elemental analyzer. The powder X-ray diffraction (XRD) pattern was recorded on a D8 X-ray diffractometer (Bruker, Germany) with Cu K α radiation ($\lambda = 1.5406$ Å). Thermal stability of SBPIL was tested using TG/DTA thermoanalyser SII, 7200 (Seiko, Japan). The sample was heated from 30 °C to 800 °C and the temperature was increased at the rate of 10 °C min⁻¹ in a nitrogen atmosphere. Thermal decomposition was taken after the weight loss of moisture from the SBPIL. Atomic absorption spectrometer (AA240, Varian, Victoria, Australia) was used to determine the unadsorbed concentration of Cr(VI).

Synthesis of SBPIL

Synthesis of 1-(4-vinylbenzyl)-1H-benzimidazole (1)

1-(4-vinylbenzyl)-1H-benzimidazole was synthesized according to the literature procedure with slight modification.²³ In a typical procedure, THF solution of 4-vinylbenzyl chloride (8.44 g, 50 mmol) was added dropwise to a stirred solution of benzimidazole (5.9 g, 50 mmol) and sodium hydride (1.2 g, 50 mmol) at 50 °C in 150 mL THF and refluxed for 48 h. The reaction mass was filtered and THF was removed by evaporation under vacuum. Dark brown oil was obtained, to which DCM was added and the organic layer was washed with deionized water (5 × 30 mL). The organic layer was dried with Na₂SO₄, filtered and the solvent was removed by



Scheme 1. Schematic representation of the synthesis of SBPIL.

evaporation to afford yellowish crystals of 1-(4-vinylbenzyl)-1H-benzimidazole (Yield 9.36 g, 80%).

¹H NMR (400 MHz, CDCl₃) δ : 7.92 (s, 1H), 7.83-7.81 (d, 2H), 7.36-7.34 (d, 2H), 7.25-7.23 (d, 2H), 7.12-7.10 (d, 2H) 6.70-6.63 (dd, 1H), 5.74-5.69 (d, 1H), 5.30 (s, 2H), 5.26-5.23 (d, 1H).

¹³C NMR (400 MHz, CDCl₃) δ : 144.02, 143.26, 137.72, 136.09, 134.90, 133.98, 127.40, 126.88, 123.19, 122.39, 120.48, 114.70, 110.13, 48.68.

Synthesis of poly(1-(4-vinylbenzyl)-1H-benzimidazole-co-styrene) (2)

A mixture of 1-(4-vinylbenzyl)-1H-benzimidazole (1) (6.084 g, 26 mmol), styrene (2.704 g, 26 mmol) and AIBN (0.0852 g, 0.52 mmol) was refluxed in 100 mL chloroform at 70 °C for 24 h under N₂ atmosphere. Chloroform was removed by evaporation under vacuum and methanol was added to the reaction mixture to afford poly(1-(4-vinylbenzyl)-1H-benzimidazole-co-styrene) as an off-white fine powder (Yield: 7.5 g, 85.34%).

¹H NMR (400 MHz, CDCl₃) δ : 7.81 (br, 1H), 7.21 (br, 2H), 6.95 (br, 2H), 6.73 (br, 4H), 6.38 (br, 5H) 5.09 (br, 2H), 1.94 (br, 2H), 1.60-1.13 (br, 1H). ¹³C NMR (400 MHz, CDCl₃) δ : 144.71, 143.96, 143.15, 134, 132.82, 132.66, 128.03, 127.35, 125.85, 122.30, 120.42, 110.05, 48.47, 44.17, 40.31, 29.71, 26.32.

Synthesis of poly(4-(1-(4-vinylbenzyl)-1H-benzimidazol-co-styrene-3-ium-3-yl)butane-1-sulphonate) (3)

7 g of poly(1-(4-vinylbenzyl)-1H-benzimidazole-co-styrene) (2) was stirred with 1,4-butane sultone (2.58 g, 19 mmol) in 150 mL chloroform at 50 °C for 48 h that resulted in the ring opening of 1,4-butane sultone. Chloroform was decanted from the reaction mixture and the remaining viscous mass was washed with diethyl ether (2 × 20 mL) followed by chloroform (2 × 20 mL). The product was allowed to dry overnight in hot air oven at 50 °C to yield a yellowish crystalline powder of poly(4-(1-(4-vinylbenzyl)-1H-benzimidazol-co-styrene-3-ium-3-yl)butane-1-sulphonate) (3).

¹H NMR (400 MHz, CDCl₃) δ : 8.40 (br, 1H), 8.09 (br, 2H), 7.64 (br, 2H), 7.13 (br, 4H), 6.44 (br, 5H) 5.38 (br, 2H), 4.54 (br, 2H), 2.61 (br, 2H), 2.06 (br, 2H), 1.72 (br, 2H), 1.05 (br, 1H), 0.89 (br, 2H).

¹³C NMR (400 MHz, CDCl₃) δ : 144.12, 143.32, 142.53, 133.61, 131.32, 130.69, 126.57, 124.59, 122.35, 121.62, 119.40, 113.91, 110.75, 50.46, 49.87, 47.49, 46.57, 45.31, 31.30, 27.62, 26.22, 22.05.

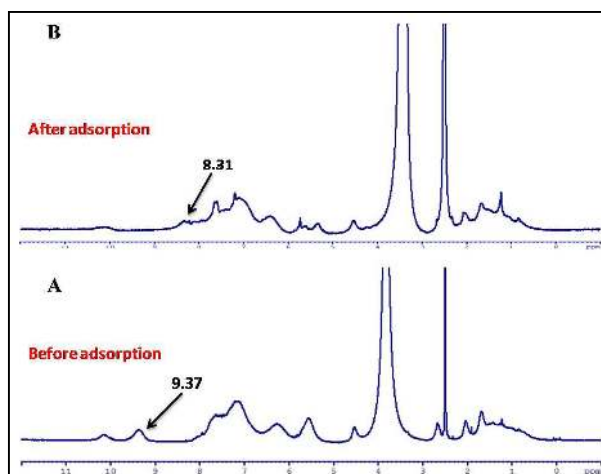


Fig. 1 ^1H NMR spectra of SBPIL (A) before and (B) after adsorption of Cr(VI).

Synthesis of SBPIL (4) from poly-(4-(1-(4-vinylbenzyl)-1H-benzimidazol-co-styrene-3-ium-3-yl)butane-1-sulphonate (3)

The poly-(4-(1-(4-vinylbenzyl)-1H-benzimidazol-co-styrene-3-ium-3-yl)butane-1-sulphonate (3) (5 g) was stirred in a minimum amount of water at ice cold condition for half an hour, after that equivalent amount (0.992 g, 9.9206 mmol) of conc. sulphuric acid was added and the stirring continued at 70 °C for 12 h. Water was decanted and the solid mass was washed with deionized water until the pH of the water (after washing) becomes neutral. The polymer was initially dried under high vacuum for 1 h followed by drying in an oven at 60 °C for 12 h, resulting in the formation of yellowish crystalline SBPIL (scheme 1). SBPIL, thus obtained was insoluble in almost all organic solvents except DMSO showing solubility at 90 °C. ^1H NMR (400 MHz, DMSO-*d*6) δ : 10.15 (br, 1H), 9.37 (br, 1H), 7.93 (br, 2H), 7.64 (br, 4H), 7.22 (br, 4H), 6.28 (br, 5H), 5.56 (br, 2H), 4.53 (br, 2H), 2.66 (br, 2H), 2.08 (br, 2H), 1.9 (br, 2H), 1.68 (br, 1H) 1.53–1.19 (br, 2H). Anal. Calcd. For $\text{C}_{30}\text{H}_{38}\text{N}_2\text{O}_7\text{S}_2$ (%): C, 56.710, H, 5.859, N, 6.436, O, 17.375, S, 7.869; Found: C, 59.86, H, 6.35, N, 4.65, O, 18.58, S, 10.64.

Adsorption studies

Batch adsorption experiments were performed in order to examine the adsorption capacities of the prepared SBPIL. A series of 100 mL Erlenmeyer flasks containing 20 mL of 50 mg L $^{-1}$ Cr(VI) solutions and 45 mg of SBPIL were shaken at 150 rpm using an orbital shaking incubator at temperature 25 ± 1 °C for 120 min. All the adsorption studies were performed at pH 5 and the pH of the solution was adjusted using 0.1 N NaOH or 0.1 N HCl. The residual concentration of Cr(VI) was determined using flame AAS.²⁴ The adsorption capacities of SBPIL were calculated using the following equation:

$$q_e = C_0 - C_e \times \frac{V}{W} \quad (1)$$

where q_e is the adsorption capacity (mg g $^{-1}$), C_0 and C_e are the initial and equilibrium concentration of Cr(VI) in the aqueous phase (mg L $^{-1}$), V is the volume of the Cr(VI) solution (L) and W is the

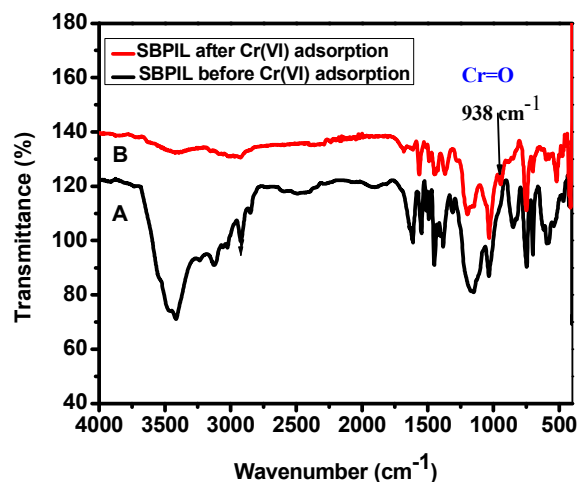


Fig. 2 FTIR spectra of SBPIL (A) before and (B) after adsorption of Cr(VI).

adsorbent dosage (g). The percentage removal of Cr(VI) was calculated from the following formula,

$$\text{Removal (\%)} = \frac{C_0 - C_e}{C_0} \times 100 \quad (2)$$

Results and discussion

Characterization of SBPIL and adsorption of Cr(VI) on SBPIL

The synthesized SBPIL and its adsorption capability towards Cr(VI) have been investigated using various spectral techniques. Fig. 1A shows the ^1H NMR spectrum of SBPIL and the corresponding spectral data has been given in the experimental section. The appearance of a new peak at δ 10.14 ppm corresponding to the $-\text{SO}_3\text{H}$ proton and the shifting of $-\text{CH}$ peak of $-\text{N}-\text{CH}=\text{N}$ in the benzimidazolium ring observed at δ 8.40 ppm in compound 3 to 9.37 ppm in compound 4, reveals that compound 3 has been successfully sulphonated to form SBPIL (4) with HSO_4^- counter ion.²⁵ However, in the presence of Cr(VI), the peak at δ 9.37 ppm once again got shifted to 8.31 ppm (Fig. 1B), which shows that HSO_4^- counter ion has been replaced from compound 4 and hence we believe that SBPIL adsorbs Cr(VI) via the replacement of HSO_4^- with HCrO_4^- .

FT-IR spectrum of SBPIL is shown in Fig. 2A which shows the characteristic broad peak for the $-\text{OH}$ stretching frequency of $-\text{SO}_3\text{H}$ group at 3452 cm^{-1} .²⁶ The peaks at 2850 and 2922 cm^{-1} correspond to the $-\text{C}-\text{H}$ groups of the aliphatic chain while the stretching frequency at 3057 and 3126 cm^{-1} is due to the $=\text{C}-\text{H}$ of the aromatic ring. The peaks at 615, 1035 and 1168 cm^{-1} correspond to the S-O symmetric vibration and S=O asymmetric and symmetric stretching frequency of the $-\text{SO}_3\text{H}$ respectively.^{27,28} In the FTIR spectrum of SBPIL after Cr(VI) adsorption (Fig. 2B), the appearance of a new peak at 938 cm^{-1} indicates the resonance peak of Cr-O and Cr=O and this confirms the presence of HCrO_4^- counter ion in SBPIL after adsorption.²⁹

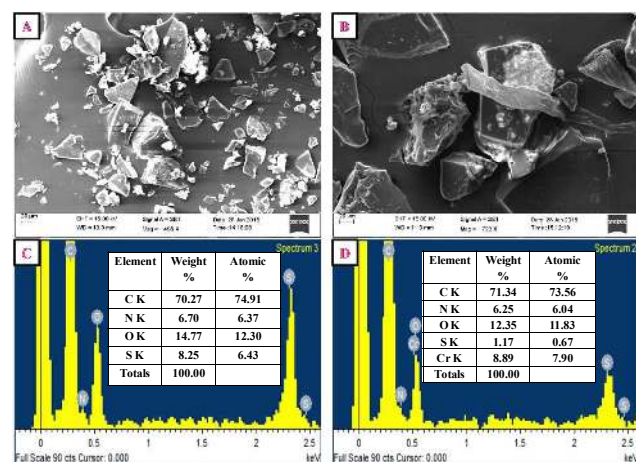


Fig. 3 SEM images of SBPIL (A) before and (B) after adsorption of Cr(VI). EDX spectra of SBPIL (C) before and (D) after adsorption of Cr(VI).

The variation in the surface morphology of SBPIL before and after adsorption of Cr(VI) were compared in Fig. 3A and 3B. Fig. 3A depicts the SEM image of synthesized SBPIL which shows a rough surface with irregularly shaped broken glass-like particles of SBPIL scattered over the surface. However, after adsorption of Cr(VI) (Fig. 3B), accumulation of tiny particles and polished surface was observed indicating the adsorption of Cr(VI) on SBPIL surface. The EDX spectrum (Fig. 3C) of SBPIL shows the presence of all expected elements in the polymer. After the adsorption of Cr(VI), new Cr peak has emerged in the region of 0.5–0.6 keV and simultaneously the intensity of S peak at 2.2–2.4 keV has significantly reduced, confirming the replacement of HSO_4^- by HCrO_4^- . Additionally, the formation of SBPIL was also confirmed using XRD and the thermal stability of SBPIL was examined using TGA (Supporting Information, Fig. S6 and S7).

Optimization of experimental parameters

As SBPIL has been found to adsorb Cr(VI) ions effectively, our next step was to optimize the experimental parameters with respect to pH, adsorbent (SBPIL) dosage and contact time for achieving maximum efficiency. The effect of pH on the adsorption of Cr(VI) on SBPIL was investigated in the pH range from 2 to 10 and the results are presented in Fig. 4A. The adsorption percentage was found to increase gradually from pH 2 to 5 and was found to decrease when the pH was increased further up to 10. Generally, Cr exists in the soluble oxide forms such as H_2CrO_4 , HCrO_4^- , $\text{Cr}_2\text{O}_7^{2-}$ and CrO_4^{2-} and the relative abundance of each species depends mainly on pH of the solution. In a highly acidic medium ($\text{pH} < 2$), H_2CrO_4 is the major species,³⁰ and it is highly difficult for H_2CrO_4 to replace the HSO_4^- from the SBPIL and hence the adsorption efficiency was found to be very less. Upon increasing the pH from 2 to 5, the availability of HCrO_4^- increases and accordingly the adsorption efficiency also increased. However, beyond pH 5, Cr(VI) is available in the form of CrO_4^{2-} ³¹ and again it becomes difficult for the CrO_4^{2-} to comfortably replace the HSO_4^- and thus there is a sudden fall in the adsorption efficiency when the pH is increased beyond 5. This study remains as an evidence for the proposed mechanism for Cr(VI)

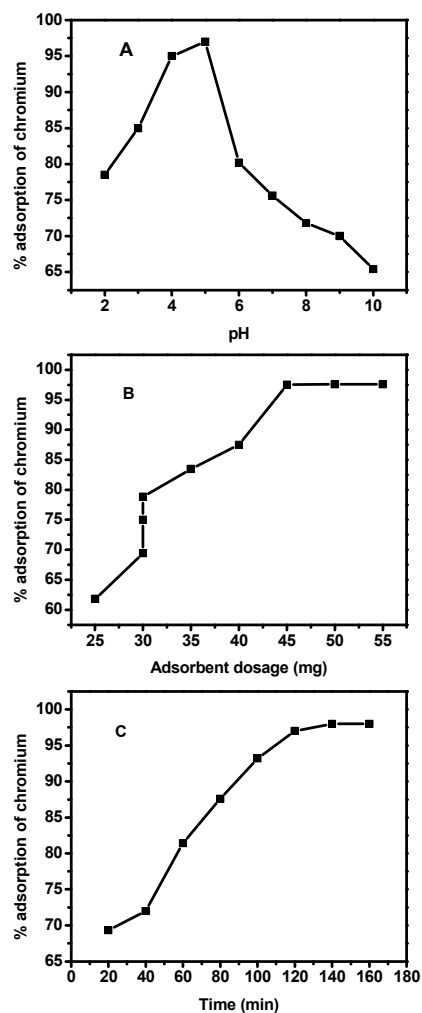


Fig. 4 Effect of (A) pH, (B) adsorbent dosage and (C) contact time on the adsorption of Cr(VI) on SBPIL.

adsorption. Since maximum adsorption was observed at pH 5, this pH was chosen as the optimum pH for further investigations.

Fig. 5B shows the adsorption efficiency of SBPIL towards Cr(VI) solutions in the presence of varying amounts of SBPIL from 25 to 55 mg. 20 mL of 50 ppm of the adsorbate used for the studies. The adsorption efficiency was found to increase upon increasing the SBPIL dosage from 25 to 45 ppm, beyond which there was no further increase. With increase in amount of the adsorbent, the number of HSO_4^- moieties are also expected to increase and thus favouring the adsorption of more amount of HCrO_4^- ions. Maximum Cr(VI) adsorption of 97.5% was achieved with 45 mg of SBPIL, and hence this amount of the adsorbent was maintained for the subsequent studies.

Similarly, the effect of contact time on the adsorption of Cr(VI) over SBPIL was also investigated (Fig. 4C). The adsorption efficiency was found to increase with time and attains the maximum at 120 min. Increase in contact time beyond 120 min, resulted in similar

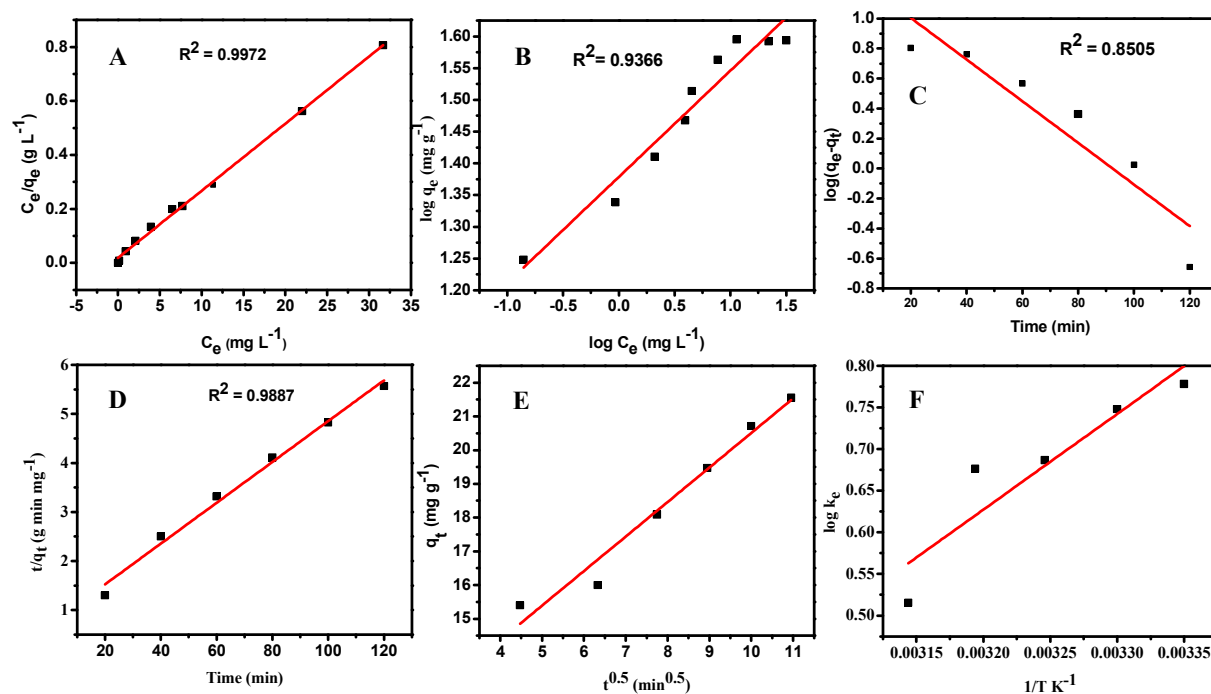


Fig. 5 (A) Langmuir isotherm (B) Freundlich isotherm (C) Pseudo-first order plot (D) Pseudo-second order plot (E) Intra particle diffusion and (F) Van't Hoff plot for the Cr(VI) adsorption on SBPIL. All the experiments were carried out with adsorbent dosage: 45 mg; pH: 5; volume of Cr(VI) solution: 20 mL and shaking rate: 160 rpm.

adsorption and thus 120 min has been chosen as the optimum contact time for the remaining studies.

Adsorption isotherm

After optimizing the experimental parameters for the adsorption of Cr(VI) on SBPIL, we were interested in understanding the adsorption behaviour. The adsorption behaviour was investigated by fitting the experimental data with Langmuir³² and Freundlich³³ adsorption isotherm models.

Langmuir adsorption states that adsorption of metal ions takes place on the homogeneous surface by monolayer adsorption without the interactions of adsorbed ions. The Langmuir adsorption isotherm can be expressed as

$$\frac{C_e}{q_e} = \frac{1}{q_0} + \frac{C_e}{q_0} \quad (3)$$

Where q_e is the amount of Cr(VI) adsorbed at equilibrium (mg g^{-1}), q_0 is the maximum adsorption capacity (mg g^{-1}), C_e is the equilibrium concentration (mg L^{-1}) and b is the Langmuir constant (L mg^{-1}). The values of q_0 and b were calculated from the slope and intercept of the plot of C_e vs C_e/q_e (Fig. 5A) and were found to be 40.8176 (mg g^{-1}) and 1.3528 (L mg^{-1}) respectively, with a correlation coefficient (R^2) is equal to 0.9972. Further, favourability of the adsorption process can be realized from the dimensionless equilibrium parameter R_L , which was calculated to be 0.061 suggesting that Langmuir adsorption isotherm was more favourable for this investigation.³⁴

Freundlich adsorption isotherm assumes that the adsorption of metal ions takes place on the heterogeneous surface by monolayer adsorption. The Freundlich adsorption isotherm is expressed as

$$\log q_e = \log K_f + \frac{1}{n} \log C_e \quad (4)$$

where q_e is the amount of Cr(VI) adsorbed at equilibrium (mg g^{-1}), C_e is the equilibrium concentration (mg L^{-1}), K_f and n are Freundlich constants which represent the adsorption capacity and intensity respectively. The value of K_f and n were found to be 3.3132 and 0.1672 (based on Fig. 5 B) which demonstrates that the adsorbent has very good affinity towards Cr(VI).³⁵

Upon fitting the experimental data with both Langmuir and Freundlich adsorption isotherm models, regression coefficients (R^2) were found to be 0.9972 and 0.9366 respectively. The higher value of regression coefficient obtained with Langmuir adsorption isotherm indicates that the experimental data correlate well with the Langmuir model. Moreover, the maximum adsorption capacity q_0 closely matches with the experimental adsorption capacity q_e in Langmuir adsorption isotherm as shown in the Table 1. This result reveals that Langmuir adsorption isotherm was followed in the adsorption of Cr(VI) on SBPIL. The adsorption capacity obtained for

Table 1 Langmuir and Freundlich isotherms for the adsorption of Cr(VI) on SBPIL.

Langmuir isotherm	Freundlich isotherm		
q_0 (mg g^{-1})	K_f ($\text{mg}^{1-1/n} \text{g}^{-1} \text{L}^{1/n}$)	40.816	3.3132
R_L	n	0.0061	0.1672
b (L mg^{-1})	R^2	1.3528	0.9366
R^2		0.9972	

Table 2 Comparison of adsorption capacities of various reported adsorbents towards Cr(VI) adsorption.

Adsorbent	Adsorption capacity (mg g ⁻¹)	References
Polyethylenimine facilitated ethyl cellulose	36.8	36
PVC-NmimCl	23.2	37
Cellulose ionic liquid blends polymeric material	38.94	38
Polymeric ionic liquid microgel beads	74	39
Activated carbon derived from acrylonitrile divinylbenzene copolymer	81.516	40
Hydrophobic poly(ionic liquid)	17.9	22
SBPIL	40.81	Present work

SBPIL towards Cr(VI) adsorption is better than or comparable with the literature reports (Table 2).

Kinetics of adsorption

In order to examine the rate controlling mechanism of the adsorption process, the obtained kinetic parameters for the adsorption of Cr(VI) on SBPIL were fitted with pseudo-first order and pseudo-second order models.^{41,42} The pseudo-first order and the pseudo-second order equations can be expressed as follows.

$$\log(q_e - q_t) = \log q_e - (K_1/2.303) \times t \quad (5)$$

$$\frac{t}{q_t} = \frac{1}{k_2 q_e^2} + \frac{t}{q_e} \quad (6)$$

where k_1 (min⁻¹) and k_2 (g mg⁻¹ min⁻¹) are the rate constants of the pseudo-first order and pseudo-second order kinetics respectively, the q_t (mg g⁻¹) and q_e (mg g⁻¹) represent the adsorption capacity at any time t (min) and at equilibrium respectively. As indicated in Fig. 5C, 5D and Table 2, regression coefficients of 0.8505 and 0.9887

Table 3 Kinetic parameters for the adsorption of Cr(VI) on SBPIL.

Pseudo-first order kinetics	k_1 (min ⁻¹)	R_1^2		
	0.0138	0.8505		
Pseudo-second order kinetics	C_0 (mg L ⁻¹)	q_e (mg g ⁻¹)	k_2 (g mg ⁻¹ min ⁻¹)	R_2^2
	50	24.038	0.0025	0.9887
	Intra-particle diffusion			
	K_{int} (mg g ⁻¹ min ^{-1/2})			
1.0231				

Table 4 Thermodynamic parameters for the adsorption of Cr(VI) on SBPIL.

Temperature T (K)	ΔG^0 (kJ/mol)	ΔS^0 (J/K mol)	ΔH^0 (kJ/mol)
298	-2.8917		
303	-3.8605		
308	-3.9841	-25.3849	-9.5624
313	-4.4121		
318	-4.6647		

were obtained for pseudo-first order and pseudo-second order kinetics respectively and this confirms that the adsorption of Cr(VI) on SBPIL follows pseudo-second order kinetic model.

Further, the intra-particle rate constant was determined using the Weber and Morris equation,

$$q_t = k_{int} \sqrt{t} + C \quad (7)$$

where k_{int} is the intra-particle diffusion constant and q_t is the amount of Cr(VI) adsorbed at time t . The k_{int} value was found to be 1.0231 mg g⁻¹ min^{-1/2} (Table 3) from the slope of the plot of q_t vs \sqrt{t} as shown in Fig. 5E. The plot obtained had a larger intercept value which can be attributed to the boundary layer effect.^{43,44} Therefore, it can be accomplished that, the intra-particle diffusion is not the only rate-controlling step, and there could be other processes that control the rate of the adsorption. Hence, the kinetics of Cr(VI) on SBPIL is likely to be controlled by the synergic effect of surface adsorption and intraparticle diffusion.

Thermodynamic study

To investigate the thermodynamics of Cr(VI) adsorption on SBPIL, the thermodynamic parameters such as standard free energy (ΔG^0), enthalpy change (ΔH^0) and entropy change (ΔS^0) were estimated by the following equations:

$$\log K_d = \frac{\Delta S^0}{2.303 R} - \frac{\Delta H^0}{2.303 RT} \quad (8)$$

$$K_d = \frac{q_e}{c_e} \quad (9)$$

where K_d is the adsorption distribution coefficient at different temperatures, R is the universal gas constant (8.314 J/mol K) and T is the absolute temperature (K). The value of ΔH^0 and ΔS^0 can be calculated from the slope and the intercept respectively, of a linear plot of $\log K_d$ against $1/T$ (Fig. 5F). The ΔG^0 values were calculated at different temperatures and the thermodynamic parameters are presented in Table 4. As indicated in the table, ΔG^0 was found to be negative at all temperatures demonstrating the spontaneous and feasible adsorption of Cr(VI) on SBPIL. Furthermore, the absolute values of ΔG^0 increases with the temperature, suggesting that Cr(VI) adsorption of SBPIL is favoured at high temperatures. The negative ΔH^0 and ΔS^0 values show that the adsorption of Cr(VI) is exothermic with decreased randomness.

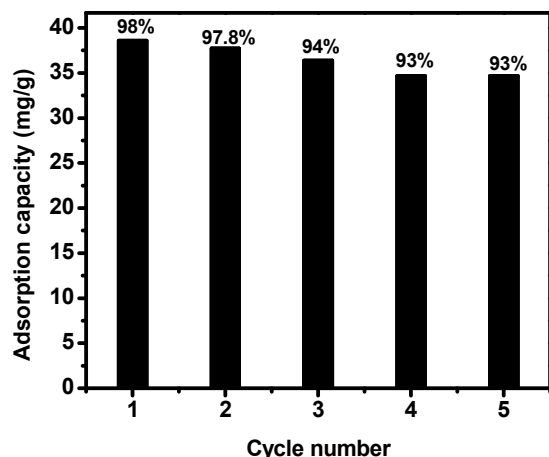


Fig. 6 Recyclability of SBPIL after Cr(VI) adsorption.

Recyclability studies

In order to investigate the efficacy of SBPIL as an adsorbent in real samples, its recyclability was tested. After adsorption of Cr(VI), SBPIL could be easily regenerated using H_2SO_4 . Cr(VI) adsorbed SBPIL was placed in the desorption medium and stirred for 180 min

at 25 °C. We have carried out the Cr(VI) desorption studies using 0.1 to 1.5 mol L^{-1} H_2SO_4 and found that the maximum desorption percentage of 98% was obtained with 1 mol L^{-1} H_2SO_4 . Fig.6 shows the ability of SBPIL towards Cr(VI) adsorption for five cycles and SBPIL was recovered using 1 mol L^{-1} H_2SO_4 after every cycle. It can be observed from the Fig. 6, there is no significant change in the Cr(VI) adsorption even after five cycles and this reveals that SBPIL can be successfully recycled and reused for Cr(VI) adsorption.

Effect of counter ions on Cr(VI) adsorption

In industrial waste water samples, Cr(VI) frequently co-exists with other anions like Cl^- , SO_4^{2-} and NO_3^- which may interfere with Cr(VI) adsorption. In order to examine the selectivity of the SBPIL, we have carried out the adsorption of Cr(VI) in the presence of equimolar concentrations (100 mg L^{-1}) of the interfering anions. We observed that Cl^- had no effect on Cr(VI) adsorption, whereas SO_4^{2-} and NO_3^- ions have diminished the Cr(VI) adsorption by 0.4% and 14.4% respectively. Further, we have increased the concentration of the interfering ions (200 mg L^{-1}) to twice that of the Cr(VI) ions. Even double the concentration of Cl^- did not have any influence on Cr(VI) adsorption whereas SO_4^{2-} and NO_3^- have reduced the adsorption by 3.6% and 19.5% respectively Fig. 7. There is no interference from Cl^- which is attributed to its lower ionic radius, and thus it is difficult for Cl^- ion to compete with the bulky HCrO_4^- in replacing the HSO_4^- . Though, SO_4^{2-} and NO_3^- are large enough to replace HSO_4^- , they differ in their hydration energy and thus NO_3^- ion (with lesser ΔG^0 of -314 kJ / mol) has major interference than that of SO_4^{2-} (with higher ($\Delta G^0 = -1103$ kJ / mol)).⁴⁵ Also, it is likely that SBPIL exhibits hydrogen bonding between C2-H of benzimidazolium cation and N of NO_3^- . The selectivity order of SBPIL is $\text{HCrO}_4^- > \text{NO}_3^- > \text{SO}_4^{2-} > \text{Cl}^-$.

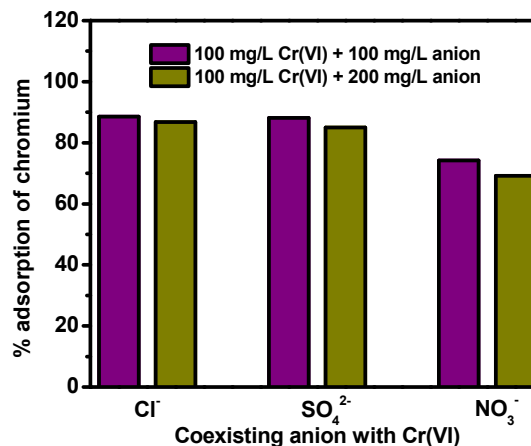


Fig. 7 Effect of co-existing anions on the adsorption of Cr(VI) adsorption on SBPIL.

Conclusions

In this work, we have carefully designed a novel benzimidazolium containing SBPIL adsorbent for efficient removal of Cr(VI) ions from water samples. The synthesized SBPIL was found to adsorb Cr(VI) through the exchange of HSO_4^- of SBPIL by HCrO_4^- and the SBPIL could be easily recovered after Cr(VI) adsorption by treatment with 1 M H_2SO_4 . The effect of pH, contact time and adsorbent dosage were investigated in order to optimize the operational conditions for maximum Cr(VI) adsorption. Maximum adsorption was achieved at pH 5 in 120 min in the presence of 45 mg of SBPIL. The adsorption isotherm fitted well with Langmuir isotherm and the kinetics of adsorption followed the pseudo-second order. Thermodynamic studies demonstrate that the Cr(VI) adsorption on SBPIL is spontaneous and exothermic. Furthermore, the SBPIL adsorbent exhibits excellent thermal stability, recyclability and reproducibility. This work may provide new approaches towards designing of polymer supported IL based adsorbents with highly tuneable and desirable characteristics.

Acknowledgements

We gratefully acknowledge SIF DST-VIT-FIST, VIT University, Vellore for providing instrumental facilities.

References

- 1 D. Mohan and C. U. Pittman Jr., *J. Hazard. Mater.*, 2006, **B137**, 762.
- 2 H. Gu, S. B. Rapole, Y. Huang, D. Cao, Z. Luo, S. Wei and Z. Guo, *J. Mater. Chem. A*, 2013, **1**, 2011–2021.
- 3 J. Esalah and M. M. Husein, *Sep. Sci. Technol.*, 2008, **43**, 3461.
- 4 M. Huebra, M.P. Elizalde and A. Almela, *Hydrometallurgy*, 2003, **68**, 33.
- 5 D. Sevdic and H. Meider, *J. Inorg. Nucl. Chem.*, 1977, **39**, 1409.
- 6 M. Koby, *Adsorpt. Sci. Technol.*, 2004, **22**, 51.
- 7 D. Mohan, K. P. Singh and V. K. Singh, *Ind. Eng. Chem. Res.*, 2005, **44**, 1027.

ARTICLE

Journal Name

- 8 V. K. Gupta A. K. Shrivastava and N. Jain, *Water Res.*, 2001, **35**, 4079.
- 9 F. Gao, H. Gu, H. Wang, X. Wang, B. Xiang and Z. Guo, *RSC Adv.*, 2015, **5**, 60208.
- 10 J. Kanagaraj, R. C. panda and V. Sumathi, *RSC Adv.*, 2015, **5**, 45300.
- 11 C. Wu, J. Fan, J. Jiang and J. Wang, *RSC Adv.*, 2015, **5**, 47165.
- 12 O. Zech, A. Stoppa, R. Buchner and W. Kunz, *J. Chem. Eng. Data*, 2010, **55**, 1774.
- 13 X. Q. Sun, H. M. Luo and S. Dai, *Chem. Rev.*, 2012, **112**, 2100.
- 14 A. P. de los Rios, F. J. Hernandez-Fernandez, L. J. Lozano, S. Sanchez, J. I. Moreno and C. Godinez, *J. Chem. Eng. Data*, 2010, **55**, 605.
- 15 R. Germani, M. V. Mancini, G. Savelli and N. Spreti, *Tetrahedron Lett.*, 2007, **48**, 1767.
- 16 M. Mincher, D. Quach, Y. Liao, B. Mincher and C. Wai, *Solvent Extr. Ion Exch.*, 2012, **30**, 735.
- 17 P. K. Mohapatra, P. Kandwal, M. Iqbal, J. Huskens, M. S. Murali and W. Verboom, *Dalton Trans.*, 2013, **42**, 4343.
- 18 N. Papaiconomou, S. Génand-Pinaz, J. M. Leveque and S. Guittonneau, *Dalton Trans.*, 2013, **42**, 1979.
- 19 A. E. Visser and R. D. Rogers, *J. Solid State Chem.*, 2003, **171**, 109.
- 20 A. E. Visser, R. P. Swatloski, W. M. Reichert, S. T. Griffin and R. D. Rogers, *Ind. Eng. Chem. Res.*, 2000, **39**, 3596.
- 21 L. w, Y. Liu, and J. Chen, *Ind. Eng. Chem. Res.*, 2009, **48**, 3261.
- 22 H. Mi, Z. Jiang and J. Kong, *Polymers*, 2013, **5**, 1203.
- 23 P. N. Muskawar, K. Thenmozhi and P. R. Bhagat, *Appl. Catal., A-Gen.*, 2015, **493**, 158.
- 24 M. I. B. Toledo, J. R. Utrilla, R. O. Perez, F. C. Marin and M. S. Polo, *Carbon*, 2014, **73**, 338.
- 25 R. Kore, T. J. Dhillip Kumar and R. Srivastava, *J. Mol. Catal. A: Chem.*, 2012, **360**, 61.
- 26 Zillillah, G. Tana and Z. Li, *Green Chem.*, 2012, **14**, 3077.
- 27 M. Vafaezadeh and M. M. Hashemi, *Chem. Eng. J.*, 2014, **250**, 35.
- 28 A. Pourjavadi, S. H. Hosseini, M. Doulabi, S. M. Fakoorpor and F. Seidi, *ACS Catal.*, 2012, **2**, 1259.
- 29 M. M. Hoffmann, J. G. Darab and J. L. Fulton, *J. Phys. Chem.*, 2001, **A105**, 1772.
- 30 Z. Ren, D. Kong, K. Wang and W. Zhang, *J. Mater. Chem. A*, 2014, **2**, 17952.
- 31 T. S. Anirudhan, S. Jalajamony and P. S. Suchithra, *Eng. Aspects*, 2009, **335**, 107.
- 32 I. Langmuir, *J. Am. Chem. Soc.*, 1918, **40 (9)**, pp. 1361.
- 33 H. M. F. Freundlich, *Z. Phys. Chem.*, 1906, **57**, pp. 385.
- 34 G. Crini, H.N. Peindy, F. Gimbert and C. Robert, *Sep. Purif. Technol.*, 2007, **53**, 97.
- 35 S. Kalidhasan, K. K. A. Santhana, V. Rajesh and N. Rajesh, *J. Hazard. Mater.*, 2012, **213–214**, 249.
- 36 B. Qui, J. Guo, X. Zhang, D. Sun, H. Gu, Q. Wang, H. Wang, X. Wang, X. Zhang, B. L. Weeks, Z. Guo and S. Wei, *ACS Appl. Mater. Interfaces*, 2014, **6**, 19816.
- 37 M. L. Chen, Y. N. Zhao, D. W. Zhang, Y. Tian and J. H. Wang, *J. Anal. At. Spectrom.*, 2010, **25**, 1688.
- 38 S. Kalidhasan, K. K. A. Santhana, V. Rajesh and N. Rajesh, *J. Colloid Interface Sci.*, 2012, **367**, 398.
- 39 Md. T. Rahman, Z. Barikbin, A. Z. M. Badruddoza, P. S. Doyle, and S. A. Khan, *Langmuir*, 2013, **29**, 9535.
- 40 D. Duranoglu, A. W. Trochimczuk, U. Beker, *Chem. Eng. J.*, 2012, **187**, 193.
- 41 H. Y. Shan, *Scientometrics*, 2004, **59**, 171.
- 42 Y. S. Ho and G. McKay, *Process Biochem.*, 1999, **34**, 451.
- 43 M. H. Entezari, N. Ghows and M. Chamsaz, *J. Phys. Chem.*, 2005, **A 109**, 4638.
- 44 E. Bulut, M. Özacar and I. Ayhan Sengil, *Microporous Mesoporous Mater.*, 2008, **115 (3)**, 234.
- 45 L. Zhu, Y. Liu, and J. Chen, *Ind. Eng. Chem. Res.*, 2009, **48**, 3261.

Graphical Abstract

Designing of sulphonic acid functionalized benzimidazolium based poly(ionic liquid) for efficient adsorption of hexavalent chromium

Avinash Ganesh Khiratkar, S. Senthil Kumar and Pundlik Rambhau Bhagat*

Department of Chemistry, School of Advanced Sciences, VIT University, Vellore-632014, India.

